

Coulomb blockade peak spacing fluctuations in deformable quantum dots: a further test to Random Matrix Theory

Raúl O. Vallejos,¹ Caio H. Lewenkopf,¹ and Eduardo R. Mucciolo²

¹ *Instituto de Física, Universidade do Estado do Rio de Janeiro,
R. São Francisco Xavier, 524, CEP 20559-900 Rio de Janeiro, Brazil*

² *Departamento de Física, Pontifícia Universidade Católica do Rio de Janeiro,
Cx.P. 38071, 22452-970 Rio de Janeiro, Brazil*

(January 17, 2018)

Abstract

We propose a mechanism to explain the fluctuations of the ground state energy in quantum dots in the Coulomb blockade regime. Employing the random matrix theory we show that shape deformations may change the adjacent peak spacing distribution from Wigner-Dyson to nearly Gaussian even in the absence of strong charging energy fluctuations. We find that this distribution is solely determined by the average number of anti-crossings between consecutive conductance peaks and the presence or absence of a magnetic field. Our mechanism is tested in a dynamical model whose underlying classical dynamics is chaotic. Our results are in good agreement with recent experiments and apply to quantum dots with spin resolved or spin degenerate states.

PACS numbers: 73.23.Hk, 05.45.+b

Most phenomena in mesoscopic electronic transport are well understood invoking the picture of a single quantum particle moving coherently in a disordered or complex potential. In the case of semiconductor quantum dots, the complexity of the background or confining potential is manifest in the chaotic nature of the underlying electronic classical dynamics. A large amount of literature [1] indicates that the statistical properties of the spectra of chaotic systems are successfully modeled by random matrix theory (RMT) [2]. When applied to transport in open ballistic quantum dots of irregular shape, this theory predicts a strong universal behavior for the statistical fluctuations of the conductance, similar to that found in disordered systems [3]. Over the last years, several experiments confirmed this behavior, making open electronic cavities one of the paradigms of quantum chaos [4,5].

Recent experiments [6,7] showed that RMT is also very successful in predicting the distribution of Coulomb blockade peaks heights in nearly isolated, many-electron quantum dots at low temperatures and zero bias [8]. In this case, the theoretical description is based on the so-called ‘constant interaction’ (CI) model [9], where the electron-electron interaction is taken into account through a fixed (capacitive) charging energy term in the Hamiltonian. The electronic many-body wave function is then formed by filling single-particle eigenstates whose fluctuations reflect the chaotic nature of the classical motion within the dot.

However, new data related to the many-body ground state energy fluctuations in these systems are at variance with the standard RMT predictions. It was observed that adjacent peak spacing energies do not fluctuate according to the celebrated Wigner surmise [10–12]. Moreover, the existence of strong correlation among the heights of nearby peaks and the apparent lack of spin degeneracy seemed to indicate that other effects, such as wave function scarring [13], interaction-induced correlations, and charging energy fluctuations [10,14,15], also play important roles.

The aim of this letter is to show that, although effects beyond the single-particle approach may be relevant to the general understanding of quantum dots, there is yet a simple mechanism based on the CI model and RMT which explains the basic feature found in Refs. [10–12], namely, the approximately Gaussian form of the peak spacing distribution. The essential point which has been missing in all previous analyses of the problem is that the gate voltage, swept to produce a series of Coulomb blockade peaks, also continuously deforms the confining potential seen by the electrons in the quantum dot [16]. As a consequence, ground state energies, which are measured from the positions of consecutive peaks, correspond to *different* parametric realizations of the one-body Hamiltonian. Since adjacent energy eigenvalues tend to lose correlation rapidly as their parametric distance increases [17], the experiments in question are likely to be measuring the spacing distribution of *uncorrelated* chaotic eigenstates. If the dot shape dependence on the gate voltage is sufficiently strong, we find that the peak spacing distribution approaches a Gaussian, regardless of the existence or not of spin degeneracy in the single-particle spectrum.

In order to present the quantitative aspects of our argument, we begin indicating the condition for the occurrence of a conductance peak within the CI model [18]:

$$E_n + nU - e\eta V_g = E_F, \quad (1)$$

where E_n is the n^{th} single-particle energy level ($n \gg 1$), U is the dot charging energy, V_g is the gate potential, and E_F is the Fermi energy (chemical potential) in the leads. The coefficient η is a function of the capacitance matrix elements of the dot [19].

In all experimental setups where plunger gates are used to define both shape and depth of the confining potential, one expects that variations in the potential V_g will continuously deform the dot. This is the actual situation at least for the experiments in Refs. [11,12]. To establish the direct relation between V_g and the dot shape we need to know the experimental set up in detail. While such study is desirable, it is not crucial for our semi-quantitative analysis and will not be pursued here. We therefore simplify the problem parametrizing the shape deformations by a generic variable X , such that $E_n = E_n(X)$.

In view of Eq. (1), the difference between the positions (in gate voltage) of two consecutive peaks is

$$\delta V_g(n) = (e\eta)^{-1}[U + E_n(X_n) - E_{n-1}(X_{n-1})]. \quad (2)$$

Subtracting the constant charging term, the single-particle contribution to the energy spacing can be written as

$$\begin{aligned} \delta E_g(n) &\equiv e\eta \delta V_g(n) - U \\ &= E_n(X_n) - E_{n-1}(X_{n-1}) + \delta E_n, \end{aligned} \quad (3)$$

with $\delta E_n = E_n(X_n) - E_n(X_{n-1})$. It is clear from Eq. (3) that the fluctuations in $\delta E_g(n)$ *should not* obey the Wigner-Dyson statistics when δE_n also fluctuates on a scale larger or of the order of the mean single-particle level spacing $\Delta = \langle E_n(X_{n-1}) - E_{n-1}(X_{n-1}) \rangle$. To understand this point, let us consider that a gate voltage variation δV_g , sufficient to add one electron to the dot, also deforms the confining potential by δX . Three illustrative situations are depicted in the single-particle spectrum shown in Fig. 1. The states indicated by the black dots fulfill Eq. (1) for different values of n . The sequence (a) corresponds to the filling of single-particle states when $\delta X = 0$, in which case the level spacings should indeed follow the Wigner-Dyson statistics. When $\delta X \neq 0$ and the deformation is moderate, we may have instead a sequence like (b). Now each filled state is slightly shifted with respect to its predecessor, level repulsion is weakened, and deviations from the Wigner-Dyson statistics begin to appear. Finally, when deformations are strong, a sequence like (c) may occur: Consecutive filled states fluctuate independently and there is hardly any sign of level repulsion. In fact, in the presence of an overall downward drift, level spacings can be “negative”.

The quantity which determines the form of the distribution of δE_g , $P(\delta E_g)$, is the ratio between δX and the typical distance between anti-crossings in parameter space, X_c . In what follows we study $P(\delta E_g)$ as a function of $\delta X/X_c$.

Peak-to-peak fluctuations in δX are of the order Δ/U and can be neglected when $U \gg \Delta$, which is the regime relevant to the experiments. Thus, let us assume that δX is independent of n . This allows us to calculate $P(\delta E_g)$ analytically in the perturbative regime. For this purpose, we model the parametric dependence of the electronic Hamiltonian as

$$H_{\text{tot}}(X + \delta X) = H + \delta X K, \quad (4)$$

where H and K are large, independent $N \times N$ matrices belonging to the proper Gaussian ensemble. The orthogonal ensemble (GOE, $\beta = 1$) is used when no magnetic field B is

present, whereas for $B \neq 0$ we use the unitary ensemble (GUE, $\beta = 2$). We use first-order perturbation theory to describe the regime of small $\delta X/X_c$ and write $\delta E_n \approx \delta X K_{nn}$. Therefore,

$$P(\delta E_g) \approx \left\langle \delta(\delta E_g - (E_n - E_{n-1} + \delta X K_{nn})) \right\rangle_{H,K}, \quad (5)$$

where $\langle \dots \rangle_{H,K}$ represents the ensemble averages over H and K . The average over K yields a Gaussian factor that depends on the first two moments of K_{nn} . We choose $\langle K_{nn} \rangle = 0$ and $\langle (K_{nn})^2 \rangle = \Delta^2/X_c^2$. The former prevents level drift, while the latter corresponds to identifying the typical distance between anti-crossings with the inverse root mean square derivative of the energy levels with respect to deformations [17], namely, $X_c = \Delta/\sqrt{\langle (dE_n/dX)^2 \rangle}$. In these terms,

$$P(\delta \varepsilon_g) \approx \left\langle \frac{1}{\sqrt{2\pi x}} \exp \left[-\frac{(\delta \varepsilon_g - \varepsilon_n + \varepsilon_{n-1})^2}{2x^2} \right] \right\rangle_H, \quad (6)$$

where $x \equiv \delta X/X_c$. For the sake of simplicity, we have rescaled all energies in units of Δ , introducing $\delta \varepsilon_g \equiv \delta E_g/\Delta$ and $\varepsilon_n = E_n/\Delta$ for all n . Since Eq. (6) depends only on the spacing between neighboring levels, the average over H can be replaced by the convolution

$$P(\delta \varepsilon_g) \approx \int_0^\infty ds P_\beta^{WD}(s) \frac{1}{\sqrt{2\pi x}} \exp \left[-\frac{(\delta \varepsilon_g - s)^2}{2x^2} \right]. \quad (7)$$

$P_\beta^{WD}(s)$ denotes the Wigner-Dyson nearest-neighbor spacing distribution (WD), corresponding to the GOE (GUE) for $\beta = 1$ ($\beta = 2$) [2]. Notice that in the limit of $x \rightarrow 0$ the Gaussian factor becomes a δ -function and $P(\delta \varepsilon_g)$ equals the WD, as expected.

The analytical evaluation of Eq. (7) is possible when we approximate the WD by the Wigner surmise $P_\beta^{WD}(s) \approx a_\beta s^\beta e^{-b_\beta s^2}$, with $a_{1(2)} = \pi/2(32/\pi^2)$ and $b_{1(2)} = \pi/4(4/\pi)$. For the GOE, introducing $\xi_1^2 \equiv \pi/4 + 1/(2x^2)$, the result is

$$P_{GOE}(\delta \varepsilon_g) \approx \frac{\pi^{1/2}}{2^{5/2} x \xi_1^2} \exp \left(-\frac{\delta \varepsilon_g^2}{2x^2} \right) \left\{ 1 + \frac{\pi^{1/2} \delta \varepsilon_g}{2x^2 \xi_1} \right. \\ \left. \times \exp \left(\frac{\delta \varepsilon_g^2}{4x^4 \xi_1^2} \right) \left[1 + \operatorname{erf} \left(\frac{\delta \varepsilon_g}{2x^2 \xi_1} \right) \right] \right\}, \quad (8)$$

whereas for the GUE, with $\xi_2^2 \equiv 4/\pi + 1/(2x^2)$, we have

$$P_{GUE}(\delta \varepsilon_g) \approx \frac{2^{5/2} \delta \varepsilon_g}{\pi^{5/2} x^3 \xi_2^4} \exp \left(-\frac{\delta \varepsilon_g^2}{2x^2} \right) \left\{ 1 + \frac{\pi^{1/2} (2x^4 \xi_2^2 + \delta \varepsilon_g^2)}{2\delta \varepsilon_g \xi_2} \right. \\ \left. \times \exp \left(\frac{\delta \varepsilon_g^2}{4x^4 \xi_2^2} \right) \left[1 + \operatorname{erf} \left(\frac{\delta \varepsilon_g}{2x^2 \xi_2} \right) \right] \right\}. \quad (9)$$

Notice that the Gaussian factor in Eq. (7) has the unsatisfactory feature that it becomes indefinitely broad for increasing values of x . This is so because the perturbation theory cannot describe consecutive anti-crossings that stabilize the level position and therefore is limited to $x \ll 1$.

We have also performed extensive numerical simulations of parametric realizations of Gaussian ensembles of $N = 500$ random matrices to obtain $P(\delta\varepsilon_g)$. For $x < 0.25$ the agreement with the analytical results is very good, with deviations becoming larger with increasing x , as expected. Moreover, only for $x < 0.25$ we have found that variations of x change significantly the shape of $P(\delta\varepsilon_g)$. The numerical results indicate that, for $x > 1$, $P(\delta\varepsilon_g)$ approaches a Gaussian distribution whose variance saturates slowly as x increases, as can be observed in Fig. 2. Thus, the utility of the analytical results is that they capture the essence of the change in shape of $P(\delta\varepsilon_g)$, ceasing to be quantitative for large values of x .

The reason why $P(\delta\varepsilon_g)$ tends to a Gaussian may be explained in the following way. First, for a sufficiently strong deformation, we expect $E_n(X_n)$ and $E_{n-1}(X_{n-1})$ to become independent. Second, we have empirically found from our simulations that the position of each level taken alone fluctuates according to a Gaussian distribution, with a certain ensemble-dependent standard deviation $\sigma_\beta \sim O(1)$. In view of Eq. (3), we conclude that

$$P(\delta\varepsilon_g)\Big|_{x \rightarrow \infty} \longrightarrow \frac{1}{\sqrt{4\pi}\sigma_\beta} \exp\left[-\frac{(\delta\varepsilon_g - 1)^2}{4\sigma_\beta^2}\right]. \quad (10)$$

(The variance of the unitary case is always smaller than the orthogonal one because the level repulsion grows with β .) We remark that some analytical work [23], as well as the Dyson Brownian motion model [2] hint the idea that the position of each level taken alone is Gaussian distributed, although we found no rigorous proof in the literature.

So far we have not considered the possibility of having spin degenerate eigenstates. In other words, the discussion focused on the case that, due to some strong exchange contribution, the mean-field solution of the many-body problem led to states with broken spin degeneracy. Let us discuss now the opposite case of spin degenerate levels, when the nearest-neighbor level spacing distribution is

$$P_\beta^{SD}(s) = \frac{1}{2}\delta(s) + \frac{1}{2}P_\beta^{WD}(s). \quad (11)$$

For $\delta X = 0$ this leads to a bimodal sequence of peaks spacings (and also of peak heights). However, in analogy to the previous discussion, as δX increases, even spin degenerate peaks will correspond to different dot shapes. Consequently, the bimodal structure will be rapidly destroyed. As δX approaches the scale of one avoided crossing, $P(\delta\varepsilon_g)$ will tend to a Gaussian. For $x > 1$ the only significant difference between the case of broken and preserved spin degeneracy is the variance of the distributions with respect to Δ , as shown in Fig. 2.

We test our mechanism by modeling the dynamics of an electron in a quantum dot using the conformal billiard [20]. The shape of the billiard is determined by the image of the circle of unit radius in the complex plane z under the conformal mapping $w(z) = (z + bz^2 + ce^{i\delta}z^3)/(1 + 2b^2 + 3c^3)^{1/2}$. We studied the case $b = 0.2$ and $c = 0.2$, sweeping the parameter δ in $[\pi/2, \pi]$. For this parameter range the conformal billiard is known to display chaotic motion in its classical limit [21]. Another convenient feature of this model is the readiness to compute eigenvalues and eigenfunctions when the billiard is threaded by an Aharonov-Bohm flux of arbitrary strength. This allows us to study the cases of preserved and broken time-reversal symmetry with equal numerical effort. We have considered eigenvalues

ordered in ascending energy ranging from the 200th up to the 250th. In this energy window, we followed the levels in parameter space to construct our histograms, observing that Δ and X_c stay almost constant over the whole energy-parameter window [22]. The scaled results are in good agreement with our theoretical predictions based on RMT. In Fig. 3 we illustrate this statement showing the case of spin resolved degeneracy.

Three experiments [10–12] have obtained peak spacing distributions that fit Gaussian curves rather well. Our results are consistent with these findings if we take $x > 1$, indicating that in the experimental setups there is at least one single-particle anti-crossing when the gate voltage is swept between peaks. Some difficulties arise when we try a more precise quantitative comparison. In particular, in Ref. [12] the authors found weak upward deviations from the Gaussian behavior at *both* tails of the distribution which cannot be reproduced within RMT and are not seen in our simulations. While the spectral statistics of the conformal billiard is rather universal, it is customary for chaotic systems to exhibit strong scarring and other non-universal features, resulting in levels that fluctuate weakly with shape deformations and do not follow RMT statistics. Although such levels are few, they may lead to deviations in the tails of $P(\delta\varepsilon_g)$. This subject is currently under investigation. Thermal smearing was also not taken into account in our analysis and may lead to a small distortion of the peak spacing distribution.

In conclusion, we have shown that the statistics of Coulomb blockade peak spacing distribution in chaotic quantum dots depends on shape deformations induced by variations in the gate voltage. Even when no fluctuations in the charging energy are present, provided that deformations are strong, the distribution of peak spacings is nearly Gaussian and quite distinct from the Wigner surmise, in qualitative accordance with experiments. We propose that the absence of spin-degeneracy bimodal structures seen in the experiments may also be caused by deformations. Although we have only considered the situation of constant charging energy in this letter, we believe that deformations should also be incorporated when wave function scarring and many-body effects beyond mean-field are present.

We thank H. Bruus for providing us with the code for diagonalizing the conformal billiard. We gratefully acknowledge the financial support of FAPERJ, CNPq, and PRONEX (Brazil).

REFERENCES

- [1] *Chaos and Quantum Physics*, edited by M. Giannoni, A. Voros, and J. Zinn-Justin (Elsevier, Amsterdam, 1991).
- [2] M. L. Mehta, *Random Matrices*, 2nd ed. (Academic Press, San Diego, 1991).
- [3] H. U. Baranger, in *Nanotechnology*, edited by G. Timp (AIP, New York, 1997).
- [4] C. W. J. Beenakker, *Rev. Mod. Phys.* **69**, 731 (1997).
- [5] T. Guhr, H. A. Weidenmüller, and A. Müller-Groeling, *cond-mat/9707301*.
- [6] A. M. Chang *et al.*, *Phys. Rev. Lett.* **76**, 1695 (1996).
- [7] J. A. Folk *et al.*, *Phys. Rev. Lett.* **76**, 1699 (1996).
- [8] R. A. Jalabert, A. D. Stone, and Y. Alhassid, *Phys. Rev. Lett.* **68**, 3468 (1992).
- [9] M. Kastner, *Rev. Mod. Phys.* **64**, 849 (1992).
- [10] U. Sivan *et al.*, *Phys. Rev. Lett.* **77**, 1123 (1996).
- [11] F. Simmel, T. Heinzl, and D. A. Wharam, *Europhys. Lett.* **38**, 123 (1997).
- [12] S. R. Patel *et al.*, *cond-mat/9708090*.
- [13] M. Stopa, *cond-mat/9709119*.
- [14] Ya. M. Blanter, A. D. Mirlin, and B. A. Muzykanstskii, *Phys. Rev. Lett.* **78**, 2449 (1997).
- [15] R. Berkovits and B. L. Altshuler, *Phys. Rev. B* **55**, 5297 (1997).
- [16] G. Hackenbroich, W. D. Heiss, and H. A. Weidenmüller, *Phys. Rev. Lett.* **79**, 127 (1997).
- [17] B. D. Simons and B. L. Altshuler, *Phys. Rev. Lett.* **70**, 4063 (1993).
- [18] C. W. J. Beenakker, *Phys. Rev. B* **44**, 1646 (1991).
- [19] L. I. Glazman and R. I. Shekhter, *J. Phys. Condens. Matter* **1**, 5811 (1989).
- [20] M. V. Berry and M. Robnik, *J. Phys. A* **19**, 649 (1986).
- [21] H. Bruus and A. D. Stone, *Phys. Rev. B* **50**, 18275 (1994).
- [22] H. Bruus, C. H. Lewenkopf, and E. R. Mucciolo, *Phys. Scrip.* **T69**, 13 (1997).
- [23] T. H. Baker and P. J. Forrester, *J. Stat. Phys.* **88**, 1371 (1997).

FIGURES

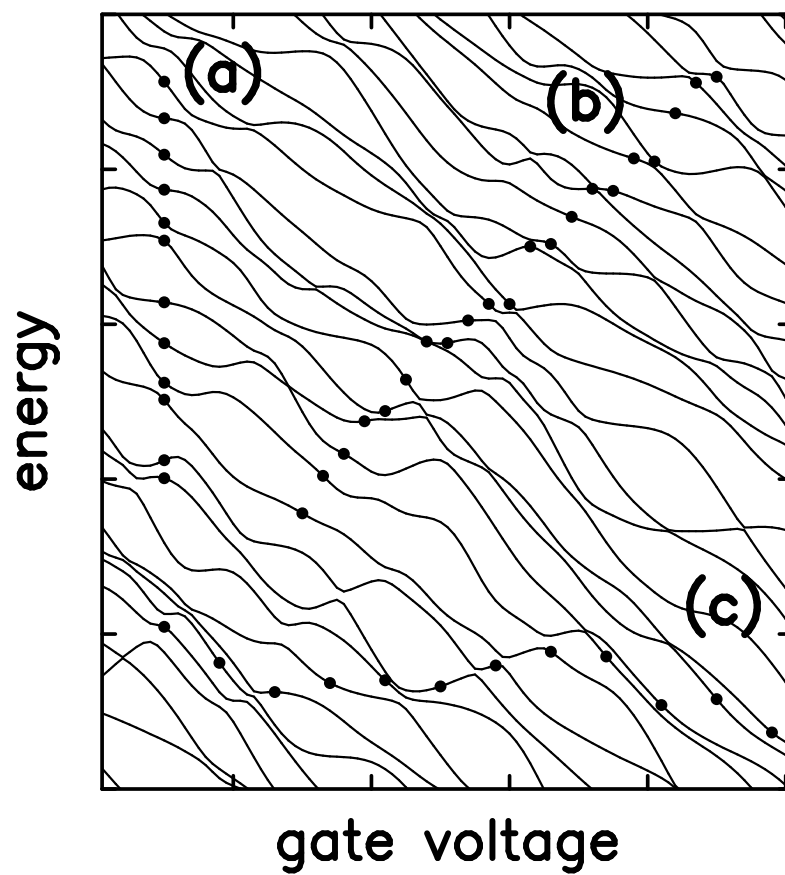


figure 1

FIG. 1. Single-particle spectrum as a function of the gate voltage (or dot shape deformation).

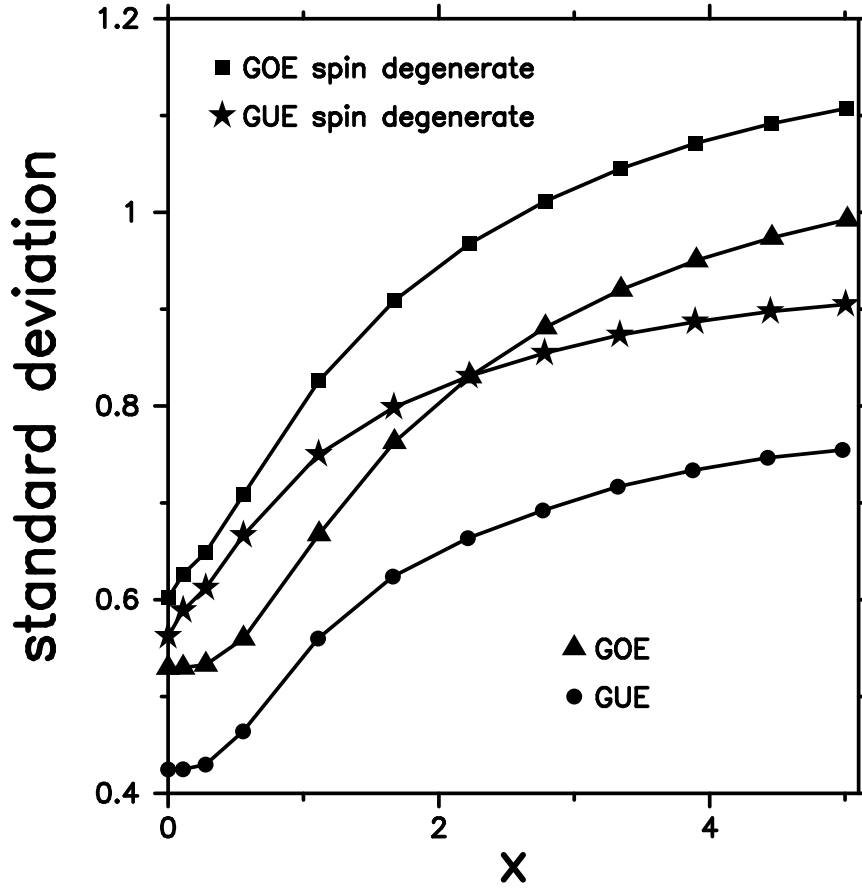


figure 2

FIG. 2. Standard deviation of $P(\delta\varepsilon_g)$ as a function of x . Squares correspond to GOE and stars to GUE for the spin degenerate case. Triangles correspond to GOE and circles to GUE for the spin resolved case.

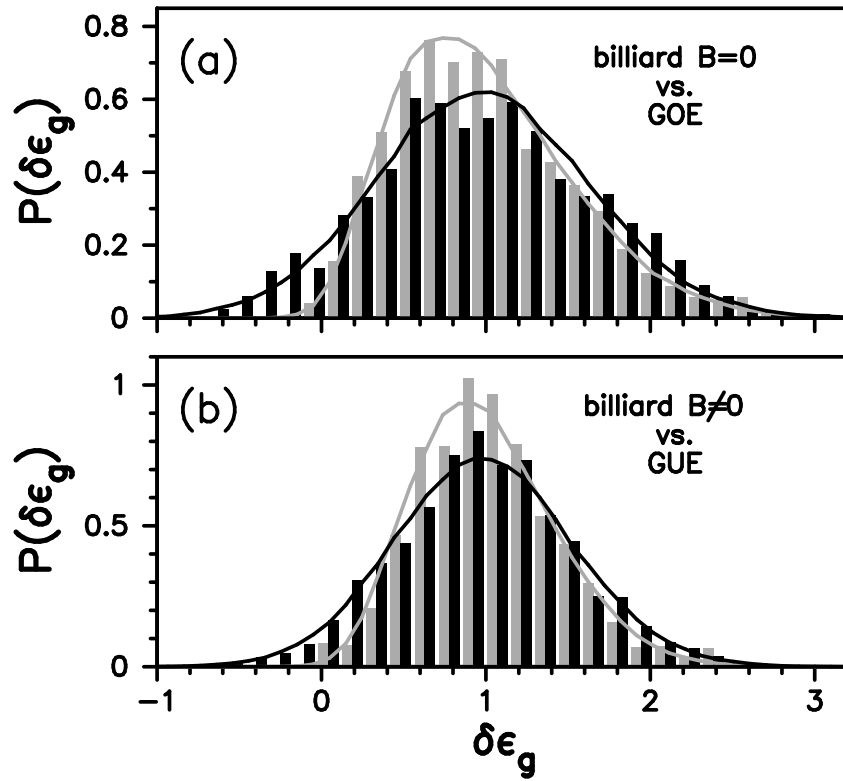


figure 3

FIG. 3. Comparison between $P(\delta\epsilon_g)$ obtained from the conformal billiard (histograms) and our numerical simulations (solid lines) for the spin resolved case: (a) GOE for $x = 0.25$ (in gray) and $x = 1$ (in black); (b) the same for GUE.